Egyptian Journal of Chemistry

Hit Identification Against Candida Albicans: Design, Synthesis, Molecular Docking and Biological Evaluation of Hybrid Styryl-Quinoxaline Based Analogues.

Aliya M. S. El Newahie[1]*, Maiy.Y.Jaballah[2], M. Alaraby Salem[3], Mohamed F. El-Badawy[4], Rabah A.T.Serya[2], Aliaa M. Kamal[1,5], and Khaled A. M. Abouzid[2*].

[1]*Department of Pharmaceutical Organic Chemistry, Faculty of Pharmacy, October University for Modern Science and Arts (MSA), Cairo, 12611, Egypt;* [2]*Department of Pharmaceutical Chemistry, Faculty of Pharmacy, Ain Shams University, Abbassia, Cairo, 11566, Egypt;* [3]*Department of Pharmaceutical Chemistry, Faculty of Pharmacy, October University for Modern Sciences and Arts (MSA), Cairo, 12611, Egypt;* [4]*Department of Microbiology and Immunology, Faculty of Pharmacy, University of Sadat City, Sadat city, Menoufia, 32897,Egypt;* [5]*Department of Pharmaceutical Organic Chemistry, Faculty of Pharmacy, Cairo University, Giza, Cairo, 11562, Egypt.*

Abstract

The occurrence of invasive fungal infections (IFIs) and the incidence of resistant fungal pathogens have increased dramatically, leading to high morbidity and mortality especially with immune-compromised patients. Owing to their multifunctional pharmacological profiles, quinoxalines attract widespread attention being a part of several biologically and technologically relevant compounds. Herein, we report the design, synthesis, structural characterization, and biological screening of a series of new quinoxaline-based scaffolds. The antimicrobial activities of the synthesized compounds were assessed against a panel of bacterial species as well as representative fungi. Interestingly, *N*-(3-chlorophenyl)-2-(3-(2-hydroxystyryl)quinoxalin-2-yl) hydrazinecarboxamide **(3a)** displayed significant antifungal activity against *Candida albicans* ($MIC_{50} \leq$ **0.25 μg/mL**) compared to that of the reference drug fluconazole (MIC_{50} =0.125 µg/mL). Molecular docking studies showed that the potency of our compounds could be attributed to the inhibition of fungal squalene epoxidase enzyme. Additionally, all synthesized compounds were almost neither toxic to human embryonic kidney cells (CC_{50} >32.0 µg/mL) nor to human red blood cells (HC_{10} >32.0 µg/mL). The above finding results suggested that compounds **3a** is a promising lead compound that merits further optimization and development as antifungal candidate.

1. Introduction

Human race has been plagued by infectious diseases throughout history. Over the past decades, fungal infections have increased theatrically affecting over 150 million cases globally and resulting in approximately 1.7 million deaths per year [1]. The excessive use of antifungal agents is accountable for multi-resistance in several fungal strains. Fungal infections endorsed by these resistant fungal microorganisms often no respond to traditional treatment to *Candida albicans*, consequently increasing the severity of illness related to this fungal infection [2]. *Candida albicans* (*C. albicans*), *Aspergillus fumigatus*, and *Cryptococcus neoformans (C. neoformans)* are examples for opportunistic fungal pathogens affecting thousands of people every year. *Candida* spp. are accountable for the majority of human fungal infections [3]. Among all *Candida* spp., *C. albicans* is responsible for a high proportion

_____

of candidiasis patients (70%~90% among all candidiasis-causing fungi) [4, 5], with mortality rate up to 43.6% due to candidemia. Among the versatile therapeutic antifungal agents (see **Figure 1**), azoles and allylamines were found to target the mevalonate pathway to block fungal sterol/ergosterol production. Azoles based antifungal agents target *Erg11p*/ *Cyp51* and disrupt the biosynthesis of ergosterol in the lanosterol demethylation step [6] leading to the accumulation of toxic sterols on the fungal cell membranes and increased levels of endogenous reactive oxygen species [7], both of which promote fungal growth arrest. Whereas, allylamines targets squalene monooxygenase (*Erg1p*) that catalyzes squalene conversion to 2, 3-oxidosqualene, a rate-limiting step of fungal ergosterol biosynthesis [8]. **[Figure 1 near Here]**
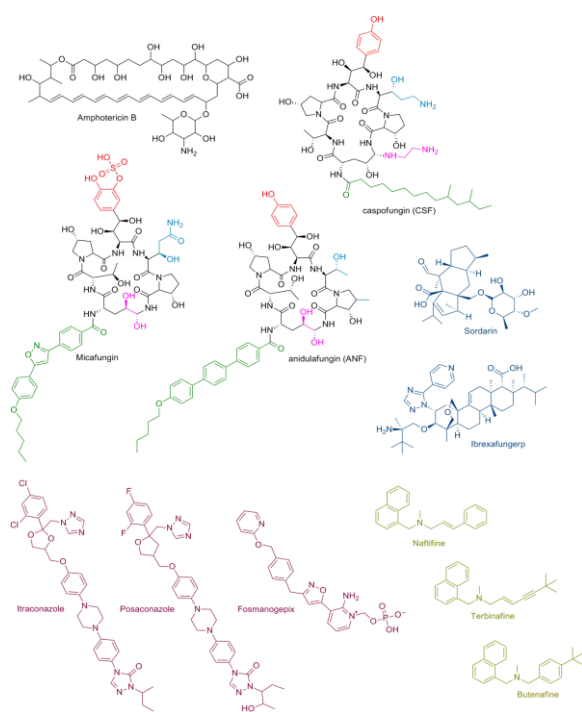
Another series of quinoxaline 1,4-di-*N*-oxides possessing *in vitro* antifungal activity against *C. albicans* (**I**, **II**, MIC_{50}=7.8 μg/mL) and *C. glabrata* (**I**, **II**, MIC_{50}=3.9 μg/mL) [10, 11], along with a series of 2,3-diphenylquinoxaline 1,4-di-*N*-oxides derivatives (**III-V**) that were useful *in-vitro* against *C. albicans* (**III / IV / V**, Zone of inhibition=15/11/10mm at 100 μg/mL), which makes them candidates for subsequent biological studies [12]. Additionally, a series of 4-aminotetrazolo[1,5-a]quinoxaline based thiazolidinone & azetidinone derivatives (**VI**, **VII**) were reported by Kumar *et al*. [13], and have exhibited good antifungal activity against *C. albicans* (Zone of inhibition 7-10 mm at 50 μg/mL) (see **Figure 2**). **[Figure 2 near here]**
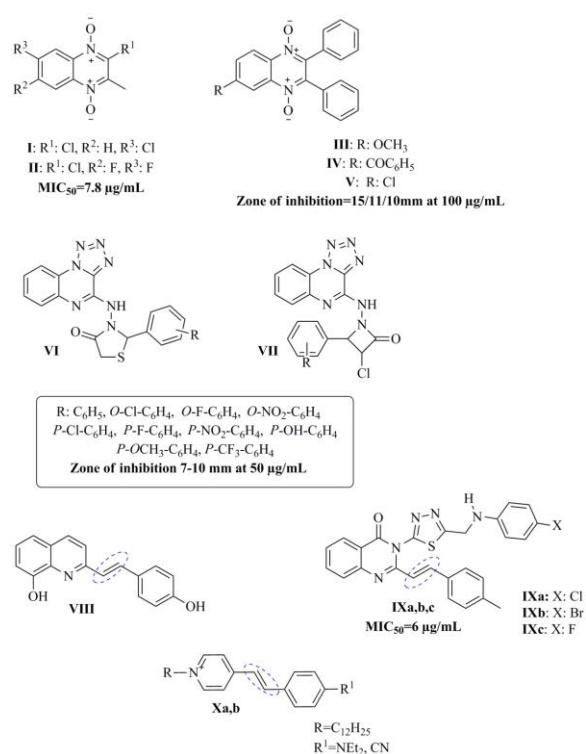

Figure 1: The structures of some antifungal drugs.

Figure 2: The structures of several reported quinoxaline and styryl-based antifungal agent.

Reduced fungal susceptibility to conventional antifungal agents and drug-resistant fungal infections poses a serious threat to continuing the treatment using conventional antifungal agents and warrants the search for new alternative molecules. In our quest for novel alternatives, we selected the styryl based quinoxaline scaffold for being reported as potential antifungal candidate in several studies. Quinoxaline-1,4-di-*N*-oxides are being identified as privileged structure in antifungal therapy with MIC_{50} range between 2 to 4 μg/mL [9].

On the other hand styryl bearing compounds have been reported as potential antifungal agents such as styryl quinolines **VIII** [14-16], styryl quinazolines **IXa-c** (which is active against *C. albicans*, MIC_{50}=6 μg/mL) [17], besides the styrylpyridinium derivatives **Xa, b** showed effective synergism with fluconazole, as well as good fungicidal activities against *C. albicans*.[18] .

Our design strategy was relied on the previously mentioned antifungal properties of quinoxaline scaffolds and styryl moieties, in addition

_____

to several reported heterocyclic structures possessing superior antifungal activity against *C. albicans* bearing benzothiazole-amide-imidazole moiety [19], along with (*E*)-(3-(substituted-styryl)-7*H*-furo[2,3-f]chromen-2-yl)(phenyl)-methanone derivatives displaying remarkable antifungal activity against *C. albicans.* [20].

The aforementioned information and the allylamines antifungal agents' structure have inspired us to synthesize a hybrid molecule combining quinoxaline ring; instead of benzothiazole, furo chromen and napthyl rings in allylamines; with a styryl moiety in position 3 of quinoxaline along with attaching aliphatic, aromatic amines or urea chain to position 2. Hence linking pharmacophoric functionalities to different aryl moieties, promises to explore antifungal activities. For better understanding of the proposed mechanism of action of our synthesized compounds, they were docked into the active site of squalene epoxidase enzyme based on structure similarity with allylamines antifungal agents.

For the pursuit of discovering new candidates that may add a value in designing new, selective, and less toxic antimicrobial agents, herein we report the design, synthesis of novel series of functionalized quinoxaline and evaluation of their antimicrobial and cytotoxicity activities along with the discovery of a novel antifungal hit compound (**3a**), (**see Figure 3**) [**Figure 3 near here**].
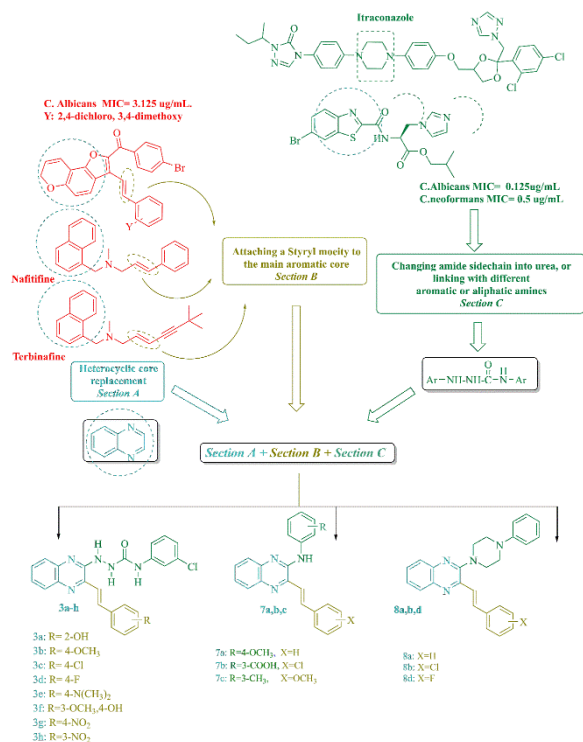

2. Material and Methods

2.1. Chemistry

All starting materials, reagents and solvents obtained from commercially available sources and used without purification. The reactions were monitored, and the purity of the compounds was checked by ascending thin layer chromatography (TLC) on silica gel-coated aluminum plates (Merck 60 F$_{254}$, 0.25 mm). Melting points were determined in open capillaries using Stuart (biocote) scientific melting point apparatus. IR spectra were determined as KBr discs using Shimadzu Infrared spectrometer (IR-435) and FT-IR 1650 (Perkin Elmer). ^{1}H NMR and ^{13}C NMR spectra were recorded in δ scale given in ppm on a Bruker 400, 100 MHz spectrophotometer. Chemical shifts have been assessed relative to the internal standard TMS and are reported in δ ppm. The coupling constants (*J*) are expressed in hertz (*Hz*) and peak multiplicities are described as singlet (*s*), doublet (*d*), triplet (*t*), quartet (*q*) and multiplet (*m*). Mass spectra were recorded on Thermo Scientific ISQLT mass spectrometer.

2-Hydrazinyl-3-methylquinoxaline (1) was prepared according to the reported method [21].

***N*-(3-chlorophenyl)-2-(3-methylquinoxalin-2-yl) hydrazine carboxamide (2)** to a hot solution of compound 1 (0.0012 mol, 0.2 g) in dry toluene (5mL), *m*-chloro phenyl isocyanate (0.0012 mol, 0.2 g) was added. The mixture was refluxed for 2 h till precipitation occurred. The precipitate was filtered while hot, washed with toluene and recrystallized from dry ethanol to afford the titled compound 2.

R$_f$= 0.6 (Hexane: EtOAc 7:3). Creamy white solid (0.33g, 88%) ; **m.p.** 233 ˚C, **^{1}H NMR (400 MHz, DMSO-*d*6) δ ppm:** 9.02 (*s*, 2H, NH, D$_2$O exchangeable), 8.42 (*s*, 1H, NH, D$_2$O exchangeable), 7.82 (*d*, *J*= 8 *Hz*, 1H, ArH), 7.72 (*s*, 1H, ArH), 7.64 (*d*, *J*= 9.6 *Hz*, 1H, ArH), 7.55 (*t*, *J*= 9.6, 7.2 *Hz*, 1H, ArH), 7.44-7.40 (*m*, 1H, ArH), 7.26 (*t*, *J*= 10.4, 6.4 *Hz*, 1H, ArH), 7.07 (*t*, *J*= 9.6, 10.8 *Hz*, 1H, ArH), 7.00 (*d*, *J*= 8 *Hz*, 1H, ArH), 2.62 (*s*, 3H, CH$_3$). **^{13}C NMR (100 MHz, DMSO-*d*6) δ ppm:** 164.0, 151.5, 143.0, 141.0, 133.0, 132.4, 130.6, 129.3, 128.1, 126.3, 125.3, 122.0, 121.9, 119.0, 21.6. **IR (KBr):** 3334 (3 NH), 3088 (CH aromatic), 2947 (CH aliphatic), 1670 (C=O), 1589 (C=C aromatic) cm^{-1}. **Anal. Calcd**. for C$_{16}$H$_{14}$ClN$_5$O (327.77): C, 58.63; H, 4.31; N, 21.37 found: C, 58.91; H, 4.47; N, 21.09.

_____

___

Standard procedure for the preparation (*E*)-*N*-phenyl-2-(styryl) quinoxalin-2-yl) hydrazine carboxamide (3a-h) (Series A)

A mixture of intermediate 2 (0.005 mol), an appropriate aldehyde (0.005 mol, 1 eq.), glacial acetic acid (**4**.5 mL) and catalytic amount of conc. sulfuric acid (0.4 mL) was refluxed for 2 h. The reaction mixture was cooled to room temperature. The separated solids were filtered, washed with water, and recrystallized from dry ethanol to afford compounds 3a-h.

(*E*)-*N*-(3-chlorophenyl)-2-(3-(2-hydroxystyryl)quinoxalin-2-yl)hydrazine-carboxamide (3a).

R_f= 0.6 (Hexane : EtOAc 7:3). Olive green solid (0.4g, 93%) ; **m.p.** > 300 °C, **^{1}H NMR (400 MHz, DMSO-d_6) δ ppm :** 9.15 (*s*, 1H, OH, D_2O exchangeable), 8.97 (*s*, 2H, NH, D_2O exchangeable), 8.75 (*d*, *J*=8 *Hz*, 1H, ArH), 8.69 (s, 1H, ArH), 8.57 (*d*, *J*=16 *Hz*, 1H, ArH), 7.88 (*d*, *J*=10 *Hz*, 1H, ArH), 7.71 (*d*, *J*=8 *Hz*, 1H, ArH), 7.62-7.37 (*m*, 5H, ArH), 7.24 (*t*, *J*=7.6, 6 *Hz*, 2H, ArH), 7.07-6.95 (*m*, 2H, CH=CH). **^{13}C NMR (100 MHz, DMSO-d_6) δ ppm :** 174.3, 157.0, 151.8, 148.9, 137.0, 136.5, 135.5, 135.2, 131.5, 130.8, 129.9, 129.1, 128.4, 126.8, 126.7, 122.8, 121.3, 120.1, 116.6, 115.4, 114.6, 113.4, 112.8. **IR (KBr):** 3300 (3 NH), 3500-3200 (OH), 3068 (CH aromatic), 2800 (CH aliphatic), 1675 (C=O), 1619-1598 (C=C aliphatic and aromatic) cm^{-1}. **Anal. Calcd.** for $C_{23}H_{18}ClN_5O_2$ (431.87): C, 63.96; H, 4.20; N, 16.22; found: C, 64.12; H, 4.36; N, 16.49.

(*E*)-*N*-(3-chlorophenyl)-2-(3-(4-methoxystyryl) quinoxalin-2-yl) hydrazine-carboxamide (3b).

R_f= 0.6 (Hexane : EtOAc 7:3). Reddish brown solid (0.4g, 85%) ; **m.p.** 256-260 °C, **^{1}H NMR (400 MHz, DMSO-d_6) δ ppm:** 13.04 (*s*, 2H, NH, D_2O exchangeable), 8.70 (*d*, *J*=8 *Hz*, 1H, ArH), 8.20 (*d*, *J*=16 *Hz*, 1H, ArH), 7.81 (*d*, *J*=8 *Hz*, 1H, ArH), 7.70 (*d*, *J*=8 *Hz*, 3H, ArH), 7.56 (*t*, *J*=8, 8 *Hz*, 2H, ArH), 7.48 (*t*, *J*=8, 8 *Hz*, 1H, ArH), 7.36 (*d*, *J*=13.6 *Hz*, 2H, CH=CH), 7.24 (*s*, 1H, ArH), 6.99 (*d*, *J*=9.2 *Hz*, 2H, ArH), 3.82 (*s*, 3H, OCH$_3$). **^{13}C NMR (100 MHz, DMSO-d_6) δ ppm:** 161.1, 154.6, 151.6, 148.4, 139.4, 136.3, 135.1, 134.1, 132.0, 131.0, 130.1, 129.9, 129.4, 129.1, 129.0, 128.4, 126.7, 119.5, 114.9, 114.6, 113.5, 55.7. **IR (KBr):** 3387 (3 NH), 3067 (CH aromatic), 2900 (CH aliphatic), 1670 (C=O), 1628-1573 (C=C aliphatic and aromatic) cm^{-1}. **Anal. Calcd.** for $C_{24}H_{20}ClN_5O_2$ (445.90): C, 64.65; H, 4.52; N, 15.71; found: C, 64.51; H, 4.68; N, 15.95.

(*E*)-*N*-(3-chlorophenyl)-2-(3-(4-chlorostyryl)quinoxalin-2-yl)hydrazine carboxamide (3c).

R_f= 0.6 (Hexane: EtOAc 7:3). Brown solid (0.4 g, 83%) ; **m.p.** 240-244 °C, **^{1}H**

NMR (400 MHz, DMSO-d_6) δ ppm: 13.06 (*s*, 2H, NH, D_2O exchangeable), 8.71 (*d*, *J*=8 *Hz*, 1H, ArH), 8.19 (*d*, *J*=16 *Hz*, 1H, ArH), 7.83, 7.81 (*dd*, *J*=8 *Hz*, 2H, ArH), 7.78, 7.76 (*dd*, *J*=8 *Hz*, 2H, ArH), 7.58 (*t*, *J*=8, 8 *Hz*, 2H, ArH), 7.51 (*d*, *J*=13.6 *Hz*, 5H, ArH and CH=CH), 7.41 (*s*, 1H, ArH). **^{13}C NMR (100 MHz, DMSO-d_6) δ ppm:** 161.5, 150.1, 149.8, 148.8, 147.5, 137.8, 137.6, 136.6, 135.3, 134.3, 132.0, 131.4, 131.0, 130.5, 129.4, 129.0, 128.1, 126.0, 124.4, 122.6, 116.1. **IR (KBr):** 3350 (3 NH), 3029 (CH aromatic), 2949 (CH aliphatic), 168 (C=O), 1627-1591 (C=C aliphatic and aromatic) cm^{-1}. **MS: m/z (%):** 454.75 [M$^+$+4, (8.23 %)], 452.34 [M$^+$+2, (8.59 %)], 450.12 [M$^+$, (12.64 %)], 279.43 (100%); **Anal. Calcd.** for $C_{23}H_{17}Cl_2N_5O$ (450.32): C, 61.34; H, 3.81; N, 15.55; found: C, 61.53; H, 3.97; N, 15.82.

(*E*)-*N*-(3-chlorophenyl)-2-(3-(4-fluorostyryl)quinoxalin-2-yl)hydrazine-carboxamide (3d).

R_f= 0.6 (Hexane: EtOAc 7:3). Yellow solid (0.39, 85%) ; **m.p.** 235- 239 °C, **^{1}H NMR (400 MHz, DMSO-d_6) δ ppm:** 13.07 (s, 2H, NH, D_2O exchangeable), 8.71, 8.68 (*dd*, *J*=12 *Hz*, 2H, ArH), 8.21 (*d*, *J*=16 *Hz*, 1H, ArH), 7.89-7.75 (*m*, 5H, ArH), 7.57 (*t*, *J*=8, 8 *Hz*, 1H, ArH), 7.48 (*t*, *J*=8, 8 *Hz*, 1H, ArH), 7.41 (*d*, *J*=20 *Hz*, 2H, CH=CH), 7.26 (*t*, *J*=8, 8 *Hz*, 2H, ArH). **^{13}C NMR (100 MHz, DMSO-d_6) δ ppm:** 188.0, 163.5, 159.5, 147.9, 142.8, 138.1, 136.3, 135.0, 132.4, 130.4, 129.5, 129.1, 126.8, 122.0, 121.9, 120.0, 116.6, 116.4, 116.0, 114.6, 107.6. **IR (KBr):** 3443 (3 NH), 3031-3071 (CH aromatic), 2907 (CH aliphatic), 1685 (C=O), 1627-1599 (C=C aliphatic and aromatic) cm^{-1}. **Anal. Calcd.** for $C_{23}H_{17}ClFN_5O$ (433.87): C, 63.67; H, 3.95; N, 16.14; found: C, 63.85; H, 4.13; N, 16.08.

(*E*)-*N*-(3-chlorophenyl)-2-(3-(4(dimethylamino)styryl)quinoxaline-2-yl)hydrazine carboxamide (3e).

R_f= 0.6 (Hexane : EtOAc 7:3). Black solid (0.42g, 84%) ; **m.p.** 245-249 °C, **^{1}H NMR (400 MHz, DMSO-d_6) δ ppm :** 8.73 (*s*, 2H, NH, D_2O exchangeable), 8.20 (*d*, *J*=13.6 *Hz*, 1H, ArH), 7.82 (*d*, *J*=8 *Hz*, 1H, ArH), 7.62 (*d*, *J*=8 *Hz*, 2H, ArH), 7.55 (*t*, *J*=8, 8 *Hz*, 2H, ArH), 7.49-7.46 (*m*, 3H, ArH), 7.37 (*s*, 1H, ArH), 7.25 (*d*, *J*=16 *Hz*, 2H, CH=CH), 6.78 (*d*, *J*=8 *Hz*, 2H, ArH), 3.02 (*s*, 6H, CH$_3$). **^{13}C NMR (100 MHz, DMSO-d_6) δ ppm :** 177.1, 158.0, 150.3,146.3, 145.0, 140.4, 137.0, 135.5, 133.0, 132.0, 130.0, 129.9, 127.2, 126.6, 125.0, 124.5, 122.0, 120.7, 118.5, 115.5, 111.7, 29.9. **IR (KBr):** 3200 (3 NH), 3148 (CH aromatic), 2890 (CH aliphatic), 1679 (C=O), 1642-1599 (C=C aliphatic and aromatic) cm^{-1}. **Anal. Calcd.** for $C_{25}H_{23}ClN_6O$ (458.94): C, 65.43; H, 5.05; N, 18.31; found: C, 65.19; H, 5.21; N, 18.47.

___

(E)-N-(3-chlorophenyl)-2-(3-(4-hydroxy-3-methoxystyryl)quinoxalin-2-yl)hydrazine carboxamide (3f). R_f= 0.6 (Hexane: EtOAc 7:3). Yellowish brown solid (0.34g, 73%) ; **m.p.** 241-245 $^{\circ}$C, **^{1}H NMR (400 MHz, DMSO-d_6) δ ppm:** 9.04 (s, 1H, OH, D_2O exchangeable), 8.71 (s, 2H, NH, D_2O exchangeable), 7.81 (d, J=8 Hz, 1H, ArH), 7.72 (s, 2H, ArH), 7.56 (t, J=8, 8 Hz, 2H, ArH), 7.47-7.37 (m, 4H, ArH and CH=CH), 7.29 (t, J=8, 8 Hz, 2H, ArH), 7.03 (d, J=8 Hz, 2H, ArH), 3.75 (s, 3H, OCH_3). **^{13}C NMR (100 MHz, DMSO-d_6) δ ppm:** 160.4, 156.2, 145.1, 143.0, 141.4, 137.1, 135.5, 133.4, 132.5, 131.4, 130.7, 130.0, 129.7, 128.0, 126.5, 125.6, 124.0, 122.3, 120.5, 119.3, 118.0, 116.1, 105.0, 56.1. **IR (KBr):** 3301 (3 NH), 3300-3100 (OH), 3082 (CH aromatic), 2900 (CH aliphatic), 1680 (C=O), 1661-1599 (C=C aliphatic and aromatic) cm^{-1}. **Anal. Calcd.** for $C_{24}H_{20}ClN_5O_3$ (461.90): C, 62.41; H, 4.36; N, 15.16; found: C, 62.65; H, 4.19; N, 15.42.

(E)-N-(3-chlorophenyl)-2-(3-(4-nitrostyryl)quinoxalin-2-yl)hydrazine-carboxamide (3g). R_f= 0.85 (Hexane : EtOAc 7:3). Brown solid (0.38g, 82%) ; **m.p.** 231-235 $^{\circ}$C, **^{1}H NMR (400 MHz, DMSO-d_6) δ ppm :** 8.83 (s, 2H, NH, D_2O exchangeable), 8.38-8.35 (m, 1H, ArH), 8.27, 8.25 (dd, J=8 Hz, 2H, ArH), 8.13-8.10 (m, 1H, ArH), 8.06, 8.04 (dd, J=8 Hz, 2H, ArH), 7.83 (d, J=8 Hz, 1H, ArH), 7.77-7.73 (m, 1H, ArH), 7.71 (d, J=17 Hz, 2H, CH=CH), 7.56 (t, J=8, 9 Hz, 1H, ArH), 7.51-7.18 (m, 3H, ArH). **IR (KBr):** 3384 (3 NH), 3075 (CH aromatic), 2901 (CH aliphatic), 1681 (C=O), 1630-1598 (C=C aliphatic and aromatic) cm^{-1}. **Anal. Calcd.** for $C_{23}H_{17}ClN_6O_3$ (460.87): C, 59.94; H, 3.72; N, 18.24; found: C, 60.12; H, 3.89; N, 18.45.

(E)-N-(3-chlorophenyl)-2-(3-(3-nitrostyryl)quinoxalin-2-yl)hydrazine-carboxamide (3h). R_f= 0.6 (Hexane : EtOAc 7:3). Red solid (0.11g, 78%) ; **m.p.** 255-257 $^{\circ}$C, **^{1}H NMR (400 MHz, DMSO-d_6) δ ppm:** 13.12 (s, 1H, NH, D_2O exchangeable), 12.97 (s, 1H, NH, D_2O exchangeable), 8.70-8.69 (m, 1H, ArH), 8.52 (s, 1H, ArH), 8.33- 8.23 (m, 2H, ArH), 8.10-7.86 (m, 3H, ArH), 7.73-7.40 (m, 4H, ArH), 7.36-6.53 (m, 3H, ArH and CH=CH). **IR (KBr):** 3397 (3 NH), 3031 (CH aromatic), 2899 (CH aliphatic), 1680 (C=O), 1632-1598 (C=C aliphatic and aromatic) cm^{-1}. **Anal. Calcd.** for $C_{23}H_{17}ClN_6O_3$ (460.87): C, 59.94; H, 3.72; N, 18.24; found: C, 60.08; H, 3.95; N, 18.41.

3-Methylquinoxalin-2-(1H)-one (4) was prepared according to the reported method. [22]

(E)-3-Styrylquinoxalin-2(1H)-one derivatives (5a-d) were prepared according to the reported method. [23-29]

(E)-2-Chloro-3-styryl-1,2-dihydroquinoxaline derivatives (6a-d) were prepared according to the reported method. [23, 26, 30]

Standard procedure for the synthesis of (E)-N-phenyl-3-styrylquinoxalin-2-amine final compounds 7a-c (Series B): To a hot solution of compounds **6a, b, c** in ethanol (15 mL), equimolar amounts of aromatic amines (0.0056 mol, 0.77 g) and catalytic amount of potassium carbonate was added, then the reaction was heated under reflux for 12 h till precipitation. The contents were cooled at room temperature. The precipitates of the compound were filtered off, washed, and recrystallized from hexane yielding final compounds **7a-c**.

(E)-N-(4-methoxyphenyl)-3-styrylquinoxalin-2-amine (7a). R_f= 0.6 (Hexane: EtOAc 7:3). Orange solid (0.29g, 82%) ; **m.p.** 250-254 $^{\circ}$C, **^{1}HNMR (400 MHz, DMSO-d_6) δ ppm:** 8.70 (s, 1H, NH, D_2O exchangeable), 8.17 (t, J=4, 4 Hz, 1H, ArH), 7.98 (t, J=4, 4 Hz, 1H, ArH), 7.75-7.69 (m, 2H, ArH), 7.50 (t, J=4, 4 Hz, 2H, ArH), 7.41 (t, J=4, 4 Hz, 2H, ArH), 7.35 (d, J=8 Hz, 2H, ArH), 7.19 (s, 1H, ArH), 7.08 (d, J=8 Hz, 2H, ArH), 6.91-6.87 (m, 2H, CH=CH), 3.77 (s, 3H, OCH_3). **IR (KBr):** 3400 (NH), 3056 (CH aromatic), 2931 (CH aliphatic), 1608-1580 (C=C aliphatic and aromatic) cm^{-1}. **Anal. Calcd.** for $C_{23}H_{19}N_3O$ (353.42): C, 78.16; H, 5.42; N, 11.89; found: C, 78.40; H, 5.66; N, 12.14.

(E)-3-((3-(4-chlorostyryl) quinoxalin-2-yl) amino) benzoic acid (7b). R_f= 0.6 (Hexane: EtOAc 7:3). Black solid (0.32g, 80%); **m.p.** 230-232 $^{\circ}$C, **^{1}H NMR (400 MHz, DMSO-d_6) δ ppm:** 10.00 (s, 1H, COOH, D_2O exchangeable), 9.00 (s, 1H, NH, D_2O exchangeable), 8.61-8.28 (m, 1H, ArH), 8.19-8.05 (m, 1H, ArH), 7.93-7.15 (m, 12H, ArH and CH=CH). **IR (KBr):** 3390 (NH), 3500-2400 (OH carboxylic), 3062 (CH aromatic), 2900 (CH aliphatic), 1696 (C=O), 1600-1541 (C=C aliphatic and aromatic) cm^{-1}. **MS: m/z (%):** 403.47 [M$^+$+2, (4.41%)], 401.43 [M$^+$, (10.98 %), 279.35 (100%); **Anal. Calcd.** for $C_{23}H_{16}ClN_3O_2$ (401.85): C, 68.74; H, 4.01; N, 10.46; found: C, 68.91; H, 4.18; N, 10.68.

(E)-3-(4-methoxystyryl)-N-(m-tolyl) quinoxalin-2-amine (7c). R_f=0.6 (Hexane : EtOAc 8:2). Orange solid (0.29 g, 82%) ; **m.p.** 150-154 $^{\circ}$C, **^{1}HNMR (400 MHz, DMSO-d_6) δ ppm :** 9.70 (s, 1H, NH, D_2O exchangeable), 8.09 (d, J=8Hz, 1H, ArH), 8.01-7.97 (m, 1H, ArH), 7.88-7.68 (m, 3H, ArH), 7.60 (t, J=8Hz, 2H, ArH), 7.33-7.31 (m, 1H, ArH), 7.21-7.07 (m, 3H, ArH), 7.02 (d, J=8Hz, 1H, ArH), 6.92-6.84 (m, 2H, CH=CH), 3.81 (s, 3H, OCH_3), 2.25 (s, 3H, CH_3). **^{13}C NMR (100 MHz, DMSO-d_6) δ ppm :** 161.1, 146.5, 140.7, 138.7,

_____

132.2, 131.7, 131.4, 130.9, 130.8, 129.4, 129.1, 128.9, 128.6, 128.4, 128.2, 127.0, 125.2, 118.9, 114.9, 114.7, 55.6, 21.2. **IR (KBr):** 3425 (NH), 3061 (CH aromatic), 2960, 2834 (CH aliphatic), 1604-1572 (C=C aliphatic and aromatic) cm^{-1}. **Anal. Calcd**. For $C_{24}H_{21}N_3O$ (367.44): C, 78.45; H, 5.76; N, 11.44; found: C, 78.68; H, 5.89; N, 11.70.

Standard procedure for the synthesis of (_E_)-2-(4-Phenylpiperazin-1-yl)-3-styrylquinoxaline final compounds 8a, b, d (Series C): To hot solution of compounds **6a, b, d** in isopropanol (15 mL), equimolar amounts of 1-phenyl piperazine (0.0056 mol, 0.77 g) and catalytic amount of triethylamine were added then the reaction was heated under reflux for 12 h till precipitation. The reaction was left to cool, and the resulted solid was filtered, washed with isopropanol, and recrystallized from benzene to give compounds **8a, b, d** in a pure form.

(_E_)-2-(4-Phenylpiperazin-1-yl)-3-styrylquinoxaline (8a). R_f= 0.6 (Hexane: EtOAc 7:3). Yellow solid (0.14g, 77%) ; **m.p.** > 300 ˚C, **^{1}H NMR (400 MHz, DMSO-_d_$_6$)** δ ppm: 7.97-7.93 (_m_, 2H, ArH), 7.83-7.80 (_m_, 1H, ArH), 7.79 (_d_, _J_=8 _Hz_, 2H, ArH), 7.68 (_t_, _J_=8, 8 _Hz_, 1H, ArH), 7.61 (_t_, _J_=8, 8 _Hz_, 1H, ArH), 7.50-7.44 (_m_, 2H, ArH), 7.40-7.37 (_m_, 2H, CH=CH), 7.26 (_t_, _J_=8, 8 _Hz_, 2H, ArH), 7.05 (_d_, _J_=8 _Hz_, 2H, ArH), 6.83 (_t_, _J_=8, 8 _Hz_, 1H, ArH), 3.53 (_s_, 4H, aliphatic), 3.45 (_s_, 4H, aliphatic). **^{13}C NMR (100 MHz, DMSO-_d_$_6$)** δ ppm: 155.1, 151.3, 145.6, 141.0, 140.1, 138.8, 136.4, 135.7, 131.5, 130.5, 129.9, 129.6, 129.5, 129.4, 128.6, 127.9, 127.3, 123.7, 119.6, 116.1, 49.9, 48.4. **IR (KBr):** 3055 (CH aromatic), 2887 (CH aliphatic), 1629-1599 (C=C aliphatic and aromatic) cm^{-1}. **Anal. Calcd.** for $C_{26}H_{24}N_4$ (392.50): C, 79.56; H, 6.16; N, 14.27; found: C, 79.42; H, 6.29; N, 14.44.

(_E_)-2-(4-Chlorostyryl)-3-(4-phenylpiperazin-1-yl) quinoxaline (8b). R_f= 0.6 (Hexane : EtOAc 7:3). Yellow solid (0.34g, 80%) ; **m.p.** 210-212 ˚C, **^{1}H NMR (400 MHz, DMSO-_d_$_6$)** δ ppm : 7.97-7.90 (_m_, 2H, ArH), 7.82 (_d_, _J_=8 _Hz_, 2H, ArH), 7.67 (_t_, _J_=8, 4 _Hz_, 1H, ArH), 7.61 (_t_, _J_=8, 8 _Hz_, 1H, ArH), 7.51-7.45 (_m_, 2H, CH=CH), 7.26 (_t_, _J_=8, 8 _Hz_, 3H, ArH), 7.04-6.97 (_m_, 2H, ArH), 6.83 (_t_, _J_=5.6, 9.6 _Hz_, 2H, ArH), 3.52 (_s_, 4H, aliphatic), 3.43 (_s_, 4H, aliphatic). **^{13}C NMR (100 MHz, DMSO-_d_$_6$)** δ ppm: 155.1, 151.4, 145.4, 140.2, 138.8, 135.4, 134.3, 133.9, 130.0, 129.6, 129.4, 128.6, 127.6, 127.3, 124.6, 121.1, 119.6, 116.1, 50.0, 48.4. **IR (KBr):** 3056 (CH aromatic), 2911 (CH aliphatic), 1628-1597 (C=C aliphatic and aromatic) cm^{-1}. **Anal. Calcd.** for $C_{26}H_{23}ClN_4$ (426.94): C, 73.14; H, 5.43; N, 13.12; found C, 73.38; H, 5.61; N, 13.40.

(_E_)-2-(4-Fluorostyryl)-3-(4-phenylpiperazin-1-yl) quinoxaline (8d). R_f= 0.6 (Hexane: EtOAc 7:3). Rose solid (0.15g, 75%) ; **m.p.** 206- 210 ˚C, **^{1}H NMR (400 MHz, DMSO-_d_$_6$)** δ ppm: 7.97 (_d_, _J_=8 _Hz_, 2H, ArH), 7.87-7.80 (_m_, 2H, ArH), 7.68 (_t_, _J_=8.4, 10.8, 1H, ArH), 7.61 (_t_, _J_=7.6, 9.2 _Hz_, 1H, ArH), 7.44 (_d_, _J_= 16 _Hz_, 2H, CH=CH), 7.28, 7.26 (_dd_, _J_=10, 8 _Hz_, 4H, ArH), 7.05 (_d_, _J_=8 _Hz_, 2H, ArH), 6.83 (_t_, _J_=8, 8 _Hz_, 1H, ArH), 3.52 (_s_, 4H, aliphatic), 3.44 (_s_, 4H, aliphatic). **^{13}C NMR (100 MHz, DMSO-_d_$_6$)** δ ppm: 151.7, 129.4, 119.4, 115.9, 51.4, 48.8, 48.6, 45.2. **IR (KBr):** 3057 (CH aromatic), 2900 (CH aliphatic), 1635-1598 (C=C aliphatic and aromatic) cm^{-1}. **Anal. Calcd.** for $C_{26}H_{23}FN_4$ (410.49): C, 76.08; H, 5.65; N, 13.65; found: C, 75.87; H, 5.77; N, 13.89.

2.2. Biological activity

Sample Preparation

The antimicrobial screening tests on bacterial and fungal strains were performed at COADD (The Community for Antimicrobial Drug Discovery), funded by the Wellcome Trust (UK) and The University of Queensland (Australia). All tested compounds were dissolved and suspended in dimethyl sulfoxide (DMSO)/ water to attain a final testing concentration of 32 μg/ml or equivalent to 20 μM. The reconstituted compounds kept at 4 °C until testing. Different eight dilutions of the tested compounds achieved by serial dilutions of 1:2 folds. The antifungal and antibacterial assays performed in non-binding surface 384-well microtitration plates, while haemolysis and cytotoxicity assays performed in propylene 384-well plate and tissue culture plates treated by mammalian cell types, respectively. All assays were performed in duplicate where DMSO did not exceed 0.5%.

Antibacterial Assay

All assessed bacterial strains were cultivated in Cation-adjusted Mueller Hinton broth (CaMHB) at 37 °C overnight. Each culture was diluted in fresh medium and incubated at 37 °C for 1.5 - 3 hr. The mid-log phase cultures were then diluted to obtain a final cell density of 5x10^5 CFU/mL in the final working volume of 50μL containing the tested compound. The micro titration plates were then incubated at 37 °C for 18 h. The absorbance was measured at 600 nm (OD$_{600}$) to determine bacterial growth inhibition using Tecan M1000 Pro monochromator plate reader. The percentage of growth inhibition was calculated for each well by the

aid of the negative control (media only) and positive control (media containing tested strain without inhibitor) on the same plate as references. The MIC_{50} was defined by an inhibition $\geq$ 80%. Hits were classified by $MIC_{50} \leq 16$ μg/mL or $MIC_{50} \leq 10$ μM in either replicate (n=2 on different plates).

Antifungal Assay

Fungal strains were cultivated on yeast extract-peptone dextrose (YPD) agar at 30 °C for 3 days. A yeast suspension of (1×10^6) to (5×10^6) CFU/mL, as determined by OD_{530}, was prepared from five colonies. The resultant suspension was diluted and added to each well of the compound-containing plates providing a final cell density of fungi suspension of 2.5×10^3 CFU/mL and a total volume of 50 μL. Afterwards, all plates were covered and incubated at 35 °C for 36 h. The growth inhibition of *C. albicans* was determined by measuring the absorbance at 630 nm (OD_{630}), after the addition of resazurin (0.001% final concentration) and incubation at 35 °C for 2 h. The absorbance was measured using a Biotek Multiflo Synergy HTX plate reader. In both cases, the growth inhibition percentage was determined for each well, using the negative control (media only) and positive control (media containing tested strain without inhibitor) in the same plate. The MIC_{50} was determined as the lowest concentration at which the growth was fully inhibited (inhibition $\geq$ 80% for *C. albicans*). Hits were classified by $MIC_{50} \leq 16$ μg/mL or $MIC_{50} \leq 10$ μM in either replicate (n=2 on different plates).

2.3. Molecular Docking

To evaluate the binding modes between compound **3a** with the target enzyme (squalene epoxidase), the molecular docking was performed using the MOE program (Chemical Computing Group software, Canada). The molecular similarity between our compounds and common squalene epoxidase inhibitors (allylamines) was the basis to choose it as the molecular target. Other fungal targets have been excluded by the basis of the absence of structural requirements for their inhibition. For instance, inhibiting the 14-α-demethylase enzyme requires interaction with the iron center in its heme moiety via azoles. [19] The geometry of the quinoxaline ring would not allow for binding with the nitrogen except in unfavorable conformations. The recently published crystal structure for the squalene

epoxidase protein makes the docking experiment more reliable than relying on homology models [31]. The crystal structure (PDB ID: 6C6P) was loaded and prepared by MOE 2020.09 using the AMBER10EHT forcefield [32]. Databases with the compounds, along with the co-crystallized ligand, have been prepared using standard preparation tools in MOE. Rigid-body docking has been applied using default parameters in MOE. Visualization was also done using the MOE software [32].
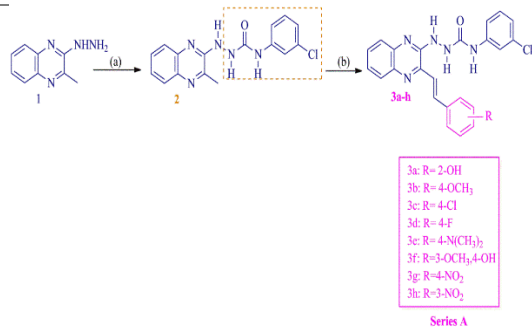
2.4. Cytotoxicity and Hemolysis Assay

At first, HEK293 cells were counted manually using Neubauer hemocytometer, and then plated in the 384-well plates containing the compounds giving density of 5×10^3 cells/ well in a final volume of 50 μL. DMEM supplemented with 10% FBS was used as growth media and the cells were incubated together with the compounds for 20 h at 37 °C in 5% CO_2. Cytotoxicity (or cell viability) was measured by fluorescence after addition of 5 μL of 25 μg/mL resazurin (2.3 μg/mL final concentrations) and incubation for further 3 h at 37 °C in 5% CO_2. Tecan M1000 Pro monochromator plate reader was used to measure the fluorescence intensity with automatic gain calculation. CC_{50} values were calculated by curve fitting the inhibition values vs. log (concentration) using a sigmoidal dose-response function. Cytotoxic samples were classified by $CC_{50} \leq 32$ μg/mL or $CC_{50} \leq 10$ μM in either replicate (n=2 on different plates).

Human whole blood was washed three times with 3 volumes of 0.9% saline and then suspended in saline to a concentration of 0.5×10^8 cells/ mL, as determined by manual cell count in a Neubauer hemocytometer. The washed cells were subsequently added to the 384 well compound-containing plates for a final volume of 50 μL followed by shaking on a plate shaker for 10 min. Afterwards, the plates were incubated for 1 h at 37 °C and centrifuged at $1000g$ for 10 min to pellet cells and debris, and then 25 μL of the supernatant was transferred to a polystyrene 384 well assay plate. Hemolysis was determined by measuring the supernatant absorbance at 405 mm (OD_{405}) using a Tecan M1000 Pro monochromator plate reader. HC_{10} and HC_{50}, defined as concentration at 10% and 50% hemolysis and were calculated by curve fitting the inhibition values *versus* log (concentration) using a sigmoidal dose-response function. Hemolysis samples were classified by $HC_{10} \leq 32$ μg/mL or $HC_{10} \leq 10$ μM in either replicate (n=2 on different plates).

_____

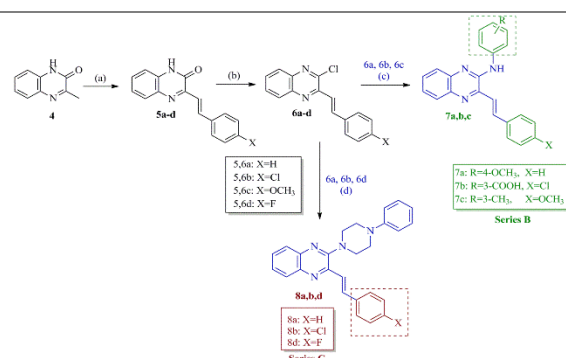### 3. Results

3.1. Chemistry

The synthetic routes of target compounds are illustrated in **Schemes 1, 2**. Urea scaffold *N*-(3-chlorophenyl)-2-(3-methylquinoxalin-2-yl) hydrazine carboxamide (**2**) has been obtained through the reaction of 2-hydrazinyl-3-methylquinoxaline (**1**) with *meta*-chlorophenyl isocyanate in dry toluene. In the present study, we planned to synthesize target styryl quinoxalines **3a-h**. For obtaining good yields of such compounds, treatment of the active methyl group of intermediate **2** with various aromatic aldehyde using acetic acid as a solvent and drops of concentrated sulphuric acid as a catalyst [23] seemed to be the most convenient approach.

Chemical structure of all obtained compounds was elucidated based on spectral techniques and elemental analysis.

Scheme 1: The synthetic routes of intermediate **2** and finals **3a-h**. Reagents and conditions: (a) 3-chlorophenylisocyanate, dry toluene, reflux, 2 h, 88 %; (b) Aromatic aldehydes, AcOH, Conc.H_2SO_4, reflux, 2 h, 73-93 %.

Scheme 2: The synthetic routes of finals **7a, b, c and 8a, b, d**. Reagents and conditions: (a) Aromatic aldehydes, AcOH, Conc.H_2SO_4, reflux, 2 h, 72-85 %; (b) $POCl_3$, reflux 1.5 h, 80-85 %; (c) Ethanol, aromatic amines, K_2CO_3, 12 h, 80-82 %; (d) Isopropanol, *N*-phenylpiperazine, TEA, reflux, 12 h, 75-80 %.

In scheme 2, we used an alternative route to prepare styryl quinoxaline starting from the condensation of 3-methylquinoxalin-2(1H)-one (**4**) with different aromatic aldehydes at first to yield (*E*)-3-styrylquinoxalin-2(1H)-one (**5a-d**). Then chlorination of the resulted intermediates **5a-d** using phosphorus oxychloride yielded the corresponding chloro compounds **6a-d** in moderate yields and melting point as reported [23, 26, 30]. Those intermediates, **6a-d,** were further utilized to obtain the corresponding substituted final series **7a, b, c** and **8a, b, d** in moderate yields through refluxing with various aromatic and aliphatic amines in different solvents (ethanol or isopropanol) using the appropriate catalysts.

_____

_____

3.2. Biological Screening

In Vitro antimicrobial activity

The antibacterial activity was examined against panel of representative Gram-negative bacteria (*E. coli*, *K. pneumonia*, *A. baumannii*, and *P.aeruginosa*) and Gram-positive bacteria [methicillin resistant *S. aureus* (MRSA)] at 32 µg/mL according to standard broth micro dilution assays [33]. Colistin and Vancomycin were used as positive bacterial inhibitor standards for Gram-negative and Gram-positive bacteria, respectively. The antifungal activity was performed against one fungal genera namely, *C. albicans* using fluconazole as a positive standard antifungal. From the obtained result, all synthesized compounds didn't exhibit any activity towards bacterial panel or *C. albicans*, however compound **3a** revealed significant inhibitory activity (**MIC₅₀ ≤ 0.25 µg/mL**) against *C. albicans* (see **Table 1 & 2**).

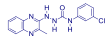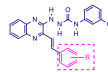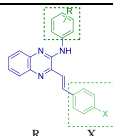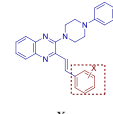**Table 1: Results of antibacterial and antifungal activities of series (A) compounds.**

Compd.	R:	Anti-bacterial *A.baum annii*	*P.aereu ginosa.*	*S.aur.*	*E.col.*	*K.pne.*	Anti-Fungal *C.alb.*
2		>32.0	>32.0	>32.0	>32.0	>32.0	>32.0
Series A							
3a	2-OH	>32.0	>32.0	>32.0	>32.0	>32.0	≤0.25
3b	4-OCH₃	>32.0	>32.0	>32.0	>32.0	>32.0	>32.0
3c	4-Cl	>32.0	>32.0	>32.0	>32.0	>32.0	>32.0
3d	4-F	>32.0	>32.0	>32.0	>32.0	>32.0	>32.0
3e	4-N(CH₃)₂	>32.0	>32.0	>32.0	>32.0	>32.0	>32.0
3f	3-OCH₃, 4-OH	>32.0	>32.0	>32.0	>32.0	>32.0	>32.0
3g	4-NO₂	>32.0	>32.0	>32.0	>32.0	>32.0	>32.0
3h	3-NO₂	>32.0	>32.0	>32.0	>32.0	>32.0	>32.0
Colistin		0.25	0.25	------	0.125	0.25	--------
Vancomycin		-------	-------	1	-------	-------	--------
Fluconazole		-------	-------	-------	-------	-------	0.125

Table 2: Results of antibacterial and antifungal activities of series (B) compounds.

Compd.	R	X	Anti-bacterial *A.baum annii*	*P.aere ginosa.*	*S.aur.*	*E.col.*	*K.pne.*	Anti-Fungal *C.alb.*
Series B								
7a	4-OCH₃	H	>32.0	>32.0	>32.0	>32.0	>32.0	>32.0
7b	3-COOH	Cl	>32.0	>32.0	>32.0	>32.0	>32.0	>32.0
7c	CH₃	OCH₃	>32.0	>32.0	>32.0	>32.0	>32.0	>32.0
Series C	X							
8a	H		>32.0	>32.0	>32.0	>32.0	>32.0	>32.0
8b	4-Cl		>32.0	>32.0	>32.0	>32.0	>32.0	>32.0
8d	4-F		>32.0	>32.0	>32.0	>32.0	>32.0	>32.0
Colistin			0.25	0.25	------	0.125	0.25	--------
Vancomycin			-------	-------	1	-------	-------	--------
Fluconazole			-------	-------	-------	-------	-------	0.125

A.bau: *Acinetobacter baumannii*.

P.aer. *Pseudomonas aeruginosa*.

S.aur. *Staphylococcus aureus*.

E.col. *Escherichia coli*.

K.pne. *Klebsiella pneumoniae*.

C.alb. *Candida albicans*.

3.3. Molecular Docking

The docking study focused on compound **3a** which showed considerable activity against *Candida albicans*. Compound **3a** shares a common pharmacophore with allylamine derivatives in terms of an aromatic center, a spacer containing H-bond acceptor, and a hydrophobic moiety. Since allylamines are known to work by the inhibition of fungal squalene epoxidase (SE), it has been chosen in this study as a possible target [34]. Although a reliable structure for the fungal SE has not been published, a recently resolved crystal structure for the human SE (**PDB ID: 6C6P**) can provide qualitative results on the possible binding mode of compound **3a**. Fortunately, as highlighted by Padyana *et al.* [31], the binding site of SE is highly conserved. The non-conserved region, which creates a difference between the binding sites in the corresponding human and fungal SE enzymes, is made up of three residues surrounding the aromatic side of the co-crystallized ligand, namely F166, I197 and L324 (see **Figure 4**).

Our aim is to compare the predicted binding pose of compound **3a** to the binding pose of terbinafine, which is a famous example of SE inhibitors. To validate the docking protocol, redocking of the co-crystallized ligand has been performed at first where it generated a pose that is nearly congruent with the co-crystallized one (see **Figure 4),** with a docking score of -15 kcal/mol. Then, terbinafine and compound **3a** were docked into the active site of human SE enzyme.
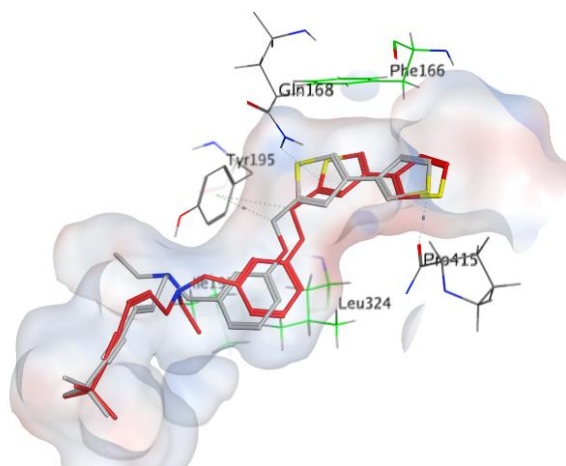

Figure 4: Overlay of the co-crystallized ligand in its original (grey) and its redocked (red) pose in the active site of squalene epoxidase (PDB ID: 6C6P). The non-conserved amino acids are shown in green lines.
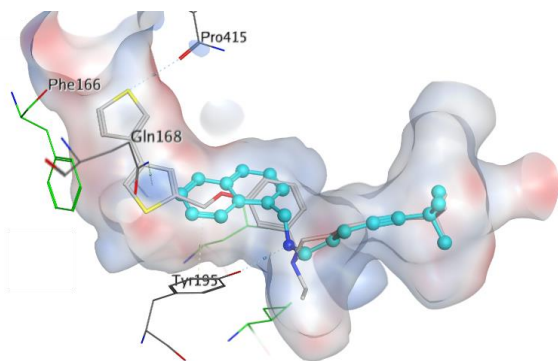

Figure 5: 3D poses of the co-crystallized ligand (grey sticks) and terbinafine (cyan ball and sticks) in the active site of squalene epoxidase (PDB ID: 6C6P). The non-conserved amino acids are shown in green lines.
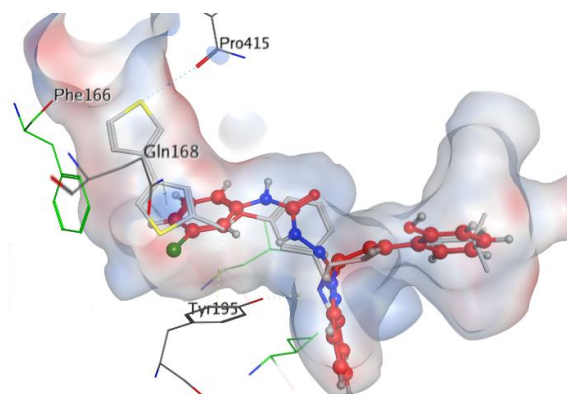

Figure 6: 3D poses of the co-crystallized ligand (grey sticks) and compound 3a (red ball and sticks) in the active site of squalene epoxidase (PDB ID: 6C6P).

3.4. Cytotoxicity against human embryonic kidney cell line and hemolysis of human red blood cells effect

To further investigate the safety profile of synthesized compounds; the final compounds were tested for their cytotoxicity against a human embryonic kidney cell line 293 (HEK293) and for hemolysis of human red blood corpuscles (RBCs) using tamoxifen and melittin as positive controls, respectively, the results were illustrated in **Table 3**. [**Table 3 near here**].

Table 3: Cytotoxicity and haemolysis ability of the tested compounds.

Compd.	CC_{50}(ug/mL)	HC_{10}(ug/mL)
2	>32.0	>32.0
3a	>32.0	>32.0
3b	>32.0	>32.0
3c	>32.0	>32.0
3d	>32.0	>32.0
3e	>32.0	>32.0
3f	>32.0	>32.0
3g	>32.0	>32.0
3h	>32.0	>32.0
7a	>32.0	>32.0
7b	>32.0	>32.0
7c	>32.0	>32.0
8a	>32.0	>32.0
8b	>32.0	>32.0
8d	>32.0	>32.0
Tamoxifen	9	NA
Melittin	NA	2.7

CC_{50} is the concentration at 50% cytotoxicity (cytotoxicity against a HEK293).

HC_{10} is the concentration at 10% haemolysis (haemolysis of human RBCs).

NA, Not Applicable.

4. Discussion

4.1. Chemistry

^{1}H NMR spectrum of intermediate **2** displayed the appearance of two singlet signals at δ 9.02 and 8.42 ppm representing the D_2O exchangeable protons of the urea group. The additional aromatic protons were proved by the appearance of singlet signal at δ 7.72 ppm. IR spectrum revealed the disappearance of the forked peak of primary amino group ($-NH_2$) and the appearance of the amidic carbonyl group (C=O) at 1670 cm^{-1}. The resulting products **3a-h** were confirmed by ^{1}H and ^{13}C NMR which revealed additional signals consistent to the introduced aromatic protons and carbons of the styryl moiety, and the disappearance of the singlet signals of aliphatic methyl ($-CH_3$) in ^{1}H NMR and ^{13}C NMR. Compounds **3a, 3f**, and **3h** displayed the appearance of multiplet signals in the range of δ 7.47-6.53 ppm corresponding to the vinylic protons. Compounds **3b**, **3c, 3d, 3e** and **3g** showed doublet signals at δ 7.36, 7.51, 7.41, 7.25, and 7.71 ppm corresponding to the vinylic protons with *J* constant 13.6, 13.6, 20.0, 16.0, and 17.0 *Hz* respectively (indicating *trans* alkene).

Compound **3a** and **3f** exhibited D_2O exchangeable singlet signal corresponding to (OH) group at δ 9.15 and 9.04 ppm, in addition to the appearance of OH broad band in IR at (3500-3200) and (3300-3100) cm^{-1} respectively. Compound **3b** showed the appearance of three methoxy protons (OCH_3) at δ 3.82 ppm in ^{1}H NMR and methoxy carbon at δ 55.7 ppm in ^{13}C NMR. Compounds **3c** and **3d** showed the appearance of doublet of doublets signals at δ 7.83, 7.78 and 8.71 ppm respectively, corresponding to the aromatic protons of the introduced styryl moiety. Compound **3e** showed the appearance of singlet signals at δ 3.02 ppm in ^{1}H NMR corresponding to six aliphatic protons (2 methyl groups) instead of 2.62 ppm representing one methyl group appeared with compound **2**. Additionally, ^{13}C NMR spectrum of compound **3e** showed a signal at δ 29.9 ppm instead of 21.6 ppm (appeared with compound **2**). A singlet signal appeared at δ 3.75 ppm in ^{1}H NMR corresponding to the three methoxy protons, in addition to a signal at δ 56.1 ppm appeared in ^{13}C NMR spectrum corresponding to methoxy (OCH_3) carbon of compound **3f**. Compound **3g** showed the appearance of doublet of doublets signals at δ 8.27 and 8.06 ppm corresponding to the introduced aromatic protons of the styryl moiety.

As for compounds **7a-7c**, ^{1}H NMR spectra revealed the appearance of new singlet signal at the range of δ 9.70- 8.70 ppm corresponding to the D_2O exchangeable proton of the secondary amine (NH-) newly formed in compounds **7a-7c** respectively, as well as the appearance of secondary amine (NH-) band in the range of 3425-3390 cm^{-1} in IR spectrum. Compounds **7b** showed the appearance of singlet signal at δ 10.00 ppm corresponding to the D_2O exchangeable proton of the newly formed carboxylic acid (-COOH). Whereas the IR spectrum of compounds **7b** showed the appearance of carboxylic band in the range of 3500-2400 cm^{-1} as well as the presence of a band at 1696 cm^{-1} corresponding to the carbonyl group of acid. Compounds **7a** showed the appearance of multiplet signals at the range of δ 6.91-6.87 ppm, whereas compound **7c** displayed a doublet signal at δ 6.92-6.84 ppm corresponding to the deshielded olefinic protons. Compound **7a** and **7c** ^{1}H NMR spectra exhibited a singlet signal at δ 3.77, 3.81 ppm corresponding to methoxy ($-OCH_3$) group. Additionally, compound **7c** showed a singlet signal at δ 2.25 ppm corresponding to methyl ($-CH_3$) group.

Considering compounds **8a,b,d**, ^{1}H NMR spectrum showed the appearance of newly formed signals corresponding to the introduced aliphatic piperazinyl protons appeared as singlets in the range of δ 3.53, 3.45 ppm for **8a**, 3.52, 3.43 ppm for **8b** and 3.52, 3.44 ppm for **8d**. ^{13}C NMR spectra showed the presence of newly formed signals corresponding to the introduced aliphatic piperazinyl carbons appeared at δ 49.9 and 48.4 ppm for **8a**, 50.0 and 48.4 ppm for **8b**, 51.4 and 48.8 ppm for **8d**. Compounds **8a** and **8b** showed the appearance of multiplet signals at the range of δ 7.51-7.37 ppm, while compound **8d** showed the appearance of doublet signal at δ 7.44 ppm corresponding to the vinylic protons with *J* constant 16 *Hz* (indicating *trans* alkene).

4.2. Biological Screening

In Vitro antimicrobial activity

To interpret the biological results, series A emerging originally from compound **2** have been investigated. Replacement of hydrogen atom in the styryl ring with hydroxyl group in position 4 (as in compounds **3f**), methoxy group in position 4 or 3 (as in compounds **3b** and **3f**), chloro, floro or dimethyl amino in position 4 (as in compounds **3c, 3d**, and **3e**) or nitro group in position 4 or 3 (as in compounds **3g** and **3h**); didn't resulted in any promising activity against *C. albicans*, yet a promising candidate emerged through substitution at position 2 of the respective styryl ring with hydroxyl group possessing impressive MIC_{50} against *C. albicans* (**MIC_{50} $\leq$ 0.25 µg/mL**). Furthermore, series B where quinoxaline is attached

_____

with different aliphatic and aromatic amines at position 2 along with a styryl moiety at position 3 also didn't develop any activity towards *C. albicans*. These results introduce compound **3a** as a promising lead compound and in the next section we shall explore its potential mechanism of action through molecular docking. [see **Table 1 & 2**].

4.3. Molecular Docking

The docking of terbinafine and compound **3a** resulted in a docking score of -10 kcal/mol. As shown in **Figure 5**, terbinafine assumes a pose that is anchored by a H-bond between the conserved Tyr195 residue and its tertiary N atom. The pose in **Figure 5** is in accordance with previous predictions by Padyana *et al.* [31]. Similarly, compound **3a** assumes a pose that involves anchoring the quinoxaline ring *via* π-π stacking with Phe495 in addition to the interaction with Tyr195. Both interactions with Tyr195 are shown as dotted lines. Interestingly, both terbinafine and **3a** do not extend in the region close to Phe166. This less extension might attribute to their decreased docking score compared to the co-crystallized ligand (-10 to -14 kcal/mol, respectively). This less binding of terbinafine to the human target, however, has been suggested to be the reason for its selectivity towards the fungal SE [31]. Based on the proposed pose for compound **3a**, it is predicted to have the same selective property as terbinafine.

4.4. Cytotoxicity against human embryonic kidney cell line and hemolysis of human red blood cells effect

From the below results, the tested compounds showed $CC_{50} > 32$ µg/mL against HEK293, which means that they are safe and non-cytotoxic compared to tamoxifen ($CC_{50}= 9$ µg/mL). Additionally, the tested compounds exhibited HC_{10} more than 32 µg/mL, so they are considered as safe and non-toxic compounds). [see **Table 3**].

5. Conclusion

Summarizing, in the current study a series of styryl-based quinoxaline scaffolds bearing arylamino or arylurea moieties were designed and synthesized based on the structural similarities with allylamines and reported antifungal agents. Compound **3a** displayed significant antifungal activity against *C. albicans* (MIC$_{50}$ **≤0.25 µg/mL**) compared to the reference drug fluconazole (MIC$_{50}$=0.125 µg/mL). Based on structure similarity with allylamines, the

predicated antifungal mechanism of compound **3a** is *via* inhibition of squalene epoxidase. The docking experiment showed similar binding modes and scores for compound **3a** and the well-known squalene epoxidase inhibitor terbinafine. Furthermore, all synthesized compounds were nearly safe to HEK293 cells (CC_{50} >32.0 µg/mL) as well as to human RBCs (HC_{10} >32.0 µg/mL). These results supported our design strategy and proudly introducing compound **3a** as a promising lead compound for the development of novel antifungal agents.

6. Conflict of Interest

The authors declare that they have no known competing financial interests or personal relationships that could have appeared to influence the work reported in this paper.

7. Formatting of funding sources

No funding sources.

8. Acknowledgment

9. References

1. Kainz K, Bauer MA, Madeo F, and Carmona-Gutierrez D (2020), Fungal infections in humans: the silent crisis. Microbial Cell 7(6): p. 143

2. Dartevelle P, Ehlinger C, Zaet A, Boehler C, Rabineau M, Westermann B, Strub J-M, Cianferani S, Haïkel Y, and Metz-Boutigue M-H (2018), D-Cateslytin: a new antifungal agent for the treatment of oral Candida albicans associated infections. Scientific reports 8(1): p. 1-10

3. Lamoth F, Lockhart SR, Berkow EL, and Calandra T (2018), Changes in the epidemiological landscape of invasive candidiasis. Journal of Antimicrobial Chemotherapy 73(suppl_1): p. i4-i13

4. Zhou PR, Hua H, and Liu XS (2017), Quantity of Candida colonies in saliva: a diagnostic evaluation for oral candidiasis. Chin J Dent Res 20(1): p. 27-32

5. Sobel JD (2007), Vulvovaginal candidosis. The Lancet 369(9577): p. 1961-1971

6. Geißel B, Loiko V, Klugherz I, Zhu Z, Wagener N, Kurzai O, van den Hondel CA, and Wagener J (2018), Azole-induced cell wall carbohydrate patches kill Aspergillus fumigatus. Nature communications 9(1): p. 1-13

7. Bhattacharya S, Esquivel BD, and White TC (2018), Overexpression or deletion of ergosterol biosynthesis genes alters doubling time, response to stress agents, and drug susceptibility in Saccharomyces cerevisiae. MBio 9(4): p. e01291-18

8. Sagatova AA (2021), Strategies to better target fungal squalene monooxygenase. Journal of Fungi 7(1): p. 49

9. Zhang H, Zhang J, Qu W, Xie S, Huang L, Chen D, Tao Y, Liu Z, Pan Y, and Yuan Z (2020), Design, Synthesis, and Biological Evaluation of Novel Thiazolidinone-Containing Quinoxaline-1, 4-di-N-oxides as Antimycobacterial and Antifungal Agents. Frontiers in chemistry 8: p. 598.

10. Carta A, Paglietti G, Nikookar MER, Sanna P, Sechi L, and Zanetti S (2002), Novel substituted quinoxaline 1, 4-dioxides with in vitro antimycobacterial and anticandida activity. European journal of medicinal chemistry 37(5): p. 355-366

11. Carta A, Loriga M, Paglietti G, Mattana A, Fiori PL, Mollicotti P, Sechi L, and Zanetti S (2004), Synthesis, anti-mycobacterial, anti-trichomonas and anti-candida in vitro activities of 2-substituted-6, 7-difluoro-3-methylquinoxaline 1, 4-dioxides. European journal of medicinal chemistry 39(2): p. 195-203

12. Leyva-Ramos S and Pedraza-Alvarez A (2021), Quinoxaline 1, 4-di-N-oxides: a review of the importance of their structure in the development of drugs against infectious diseases and cancer. Medicinal Chemistry Research: p. 1-10

13. Kumar S, Khan S, Alam O, Azim R, Khurana A, Shaquiquzzaman M, Siddiqui N, and Ahsan W (2011), Synthesis of tetrazolo [1, 5-a] quinoxaline based azetidinones & thiazolidinones as potent antibacterial & antifungal agents. Bulletin of the Korean Chemical Society 32(7): p. 2260-2266.

14. Musiol R (2020), Styrylquinoline–A Versatile Scaffold in Medicinal Chemistry. Medicinal Chemistry 16(2): p. 141-154.

15. Szczepaniak J, Cieślik W, Romanowicz A, Musioł R, and Krasowska A (2017), Blocking and dislocation of Candida albicans Cdr1p transporter by styrylquinolines. International journal of antimicrobial agents 50(2): p. 171-176.

16. Cieslik W, Szczepaniak J, Krasowska A, and Musiol R (2020), Antifungal styryloquinolines as Candida albicans efflux pump inhibitors: styryloquinolines are ABC transporter inhibitors. Molecules 25(2): p. 345.

17. Sahu A, Patel A, and Sahoo HB (2020), New Derivatives of (E)-3-(5-((substitutedphenylamino) methyl)-1, 3, 4-thiadiazol-2-yl)-2-styryl quinazolin-4 (3H)-one: Searching for New Antifungal and Antibacterial Agents. International Journal of Pharmaceutical & Biological Archives 11(2): p. 76-90

18. Vaitkienė S, Kuliešienė N, Sakalauskaitė S, Bekere L, Krasnova L, Vigante B, Duburs G, and Daugelavičius R (2021), Antifungal activity of styrylpyridinium compounds against Candida albicans. Chemical Biology & Drug Design 97(2): p. 253-265

19. Zhao S, Zhao L, Zhang X, Liu C, Hao C, Xie H, Sun B, Zhao D, and Cheng M (2016), Design, synthesis, and structure-activity relationship studies of benzothiazole derivatives as antifungal agents. European Journal of Medicinal Chemistry 123: p. 514-522.

20. Boddupally S, Jyothi P, Rao MVB, and Rao KP (2019), Design and Synthesis of Antimicrobial Active (E)-(3-(Substituted-styryl)-7H-furo [2, 3-f] chromen-2-yl)(phenyl) methanone Derivatives and Their In Silico Molecular Docking Studies. Journal of Heterocyclic Chemistry 56(1): p. 73-80

21. Wagle S, Adhikari AV, and Kumari NS (2009), Synthesis of some new 4-styryltetrazolo [1, 5-a] quinoxaline and 1-

_____

substituted-4-styryl [1, 2, 4] triazolo [4, 3-a] quinoxaline derivatives as potent anticonvulsants. European journal of medicinal chemistry 44(3): p. 1135-1143.

22. Singh DP, Deivedi SK, Hashim SR, and Singhal RG (2010), Synthesis and antimicrobial activity of some new quinoxaline derivatives. Pharmaceuticals 3(8): p. 2416-2425

23. Noolvi MN, Patel HM, Bhardwaj V, and Chauhan A (2011), Synthesis and in vitro antitumor activity of substituted quinazoline and quinoxaline derivatives: search for anticancer agent. European journal of medicinal chemistry 46(6): p. 2327-2346.

24. Hao X, Qin X, Zhang X, Ma B, Qi G, Yu T, Han Z, and Zhu C (2019), Identification of quinoxalin-2 (1 H)-one derivatives as a novel class of multifunctional aldose reductase inhibitors. Future medicinal chemistry 11(23): p. 2989-3004

25. Husain A, Madhesia D, Rashid M, Ahmad A, and Khan SA (2016), Synthesis and in vivo diuretic activity of some new benzothiazole sulfonamides containing quinoxaline ring system. Journal of enzyme inhibition and medicinal chemistry 31(6): p. 1682-1689.

26. Patel HM, Bhardwaj V, Sharma P, Noolvi MN, Lohan S, Bansal S, and Sharma A (2019), Quinoxaline-PABA bipartite hybrid derivatization approach: Design and search for antimicrobial agents. Journal of Molecular Structure 1184: p. 562-568.

27. Mahajan S, Slathia N, Nuthakki VK, Bharate SB, and Kapoor KK (2020), Malononitrile-activated synthesis and anti-cholinesterase activity of styrylquinoxalin-2 (1 H)-ones. RSC Advances 10(27): p. 15966-15975.

28. Slathia N, Gupta A, and Kapoor KK (2021), Intramolecular oxidative rearrangement: I2/TBHP/DMSO-mediated metal free facile access to quinoxalinone derivatives. Tetrahedron Letters 78: p. 153268

29. Liu Z, Yu S, Di Chen GS, Wang Y, Hou L, Lin D, Zhang J, and Ye F (2016), Design, synthesis, and biological evaluation of 3-vinyl-quinoxalin-2 (1H)-one derivatives as novel antitumor inhibitors of FGFR1. Drug design, development and therapy 10: p. 1489

30. Lippmann e and Baumgartl m (1980), quinoxalines. xii. synthesis and reactions of 3-methyl-6-nitro-1h-quinoxalin-2-one derivatives. chemischer informationsdienst 11(22).

31. Padyana AK, Gross S, Jin L, Cianchetta G, Narayanaswamy R, Wang F, Wang R, Fang C, Lv X, and Biller SA (2019), Structure and inhibition mechanism of the catalytic domain of human squalene epoxidase. Nature communications 10(1): p. 1-10

32. Tarbeeva DV, Krylova NV, Iunikhina OV, Likhatskaya GN, Kalinovskiy AI, Grigorchuk VP, Shchelkanov MY, and Fedoreyev SA (2022), Biologically active polyphenolic compounds from Lespedeza bicolor. Fitoterapia: p. 105121

33. Frei A, Zuegg J, Elliott AG, Baker M, Braese S, Brown C, Chen F, Dowson CG, Dujardin G, and Jung N (2020), Metal complexes as a promising source for new antibiotics. Chemical science 11(10): p. 2627-2639

34. Nowosielski M, Hoffmann M, Wyrwicz LS, Stepniak P, Plewczynski DM, Lazniewski M, Ginalski K, and Rychlewski L (2011), Detailed mechanism of squalene epoxidase inhibition by terbinafine. Journal of chemical information and modeling 51(2): p. 455-462